Simulation of quantum-state endoscopy

P. J. Bardroff, E. Mayr, and W. P. Schleich
Abteilung für Quantenphysik, Universität Ulm, D-89069 Ulm, Germany

P. Domokos,* M. Brune, J. M. Raimond, and S. Haroche
Laboratoire Kastler Brossel, Département de Physique, Ecole Normale Supérieure, 24 rue Lhomond, F-75231 Paris Cedex, France
(Received 6 October 1995)

We demonstrate the experimental feasibility of quantum-state endoscopy [P. J. Bardroff, E. Mayr, and W. P. Schleich, Phys. Rev. A **51**, 4963 (1995)] to measure the complete quantum state of a single mode of the electromagnetic field in a cavity. We perform numerical simulations of an experiment in progress.

PACS number(s): 42.50.−p, 03.65.Bz, 84.40.Ik

In a recent paper [1] we proposed the method of quantum-state endoscopy to measure the complete quantum state of a single mode of the electromagnetic field. In the present paper we perform numerical simulations of an experimental realization of this scheme based on realistic parameters [2]. To keep the paper self-contained we first briefly summarize the essential features of this method and then study the influence of various sources of errors. We show that the currently available experimental techniques allow us to reconstruct the field state in the cavity—even for a Schrödinger cat state [3,4].

Figure 1 shows a possible experimental realization of quantum-state endoscopy. Atoms from a thermal Rb beam are promoted in region P by laser excitation and microwave transfer [5] to the circular Rydberg state $|e\rangle$ with principal quantum number 51. The atoms then interact with a classical field F, preparing a coherent superposition

$$|\phi\rangle = \sin\left(\omega\frac{l}{v}\right)|e\rangle - e^{i\varphi}\cos\left(\omega\frac{l}{v}\right)|g\rangle$$

of $|e\rangle$ and $|g\rangle$ with principal quantum number 50. The frequency of the $|e\rangle$-$|g\rangle$ transition is 51.099 GHz. Here ω is the Rabi frequency associated with the classical field of effective interaction length l, v denotes the atomic velocity, and φ is the relative internal phase of the atom. The as-prepared atom interacts with the field of the cavity C. We use the same microwave source S to prepare the atomic state and the field inside the cavity. By shifting the phase of the classical field F relative to the cavity field using a dephaser D we are able to adjust the phase φ of the atomic superposition. After the interaction the internal state of the atom is detected. From the number of atoms exiting the cavity in the excited state we are able to calculate the photon-number probability amplitudes w_n of the initial cavity field state

$$|\psi\rangle = \sum_{n=0}^{\infty} w_n |n\rangle. \tag{1}$$

We emphasize that in this method the field state has to be prepared identically before each atom enters the cavity. Moreover, we note that the method in its present form only works for pure states [6].

The central quantity in the method of quantum-state endoscopy is the probability P_e for an atom to leave the cavity in the excited state. In order to find P_e we describe the interaction of the quantized field and the resonant two-level atom by the well-known Jaynes-Cummings model. We neglect damping of the field inside the resonator, because the maximal interaction time (40 μs) is much shorter than the lifetime of the field energy in the cavity (up to 5 ms). We also neglect the decay of the atomic states, because the transit time of the atom across the apparatus (600 μs) is much shorter than the radiative decay time (30 ms). This model immediately provides the probability [1]

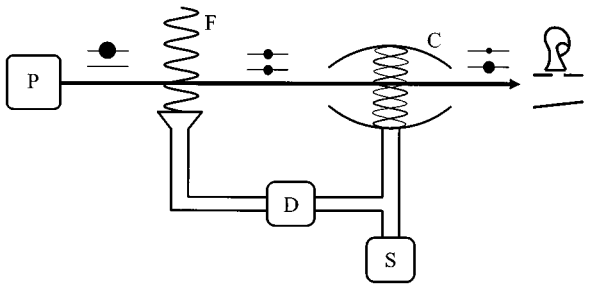

FIG. 1. Schematic illustration of quantum-state endoscopy. A classical microwave field F prepares a circular Rydberg atom in a coherent superposition of excited state $|e\rangle$ ($n=51$) and ground state $|g\rangle$ ($n=50$). The atom interacts then with a single mode of the radiation field, which is in a pure quantum state described by photon-number probability amplitudes w_n. A source S prepares the field C and generates the classical field F. A dephaser D allows us to adjust the relative phase φ. We probe the internal state of the atom leaving the cavity via state selective field ionization. We record the atomic population $P_e(t,\varphi)$ in the excited state as a function of atom-cavity interaction time t and phase φ.

*Permanent address: Crystal Physics Laboratory, Hungarian Academy of Science, P.O. Box 132, H-1504, Hungary.

$$P_e\left(t=\frac{L}{v},\varphi\right)=\frac{1}{2}+\frac{1}{2}\sum_{n=0}^{\infty}\left[\cos\left(2\Omega_n\frac{L}{v}\right)\sin^2\left(\omega\frac{l}{v}\right)-\cos\left(2\Omega_{n-1}\frac{L}{v}\right)\cos^2\left(\omega\frac{l}{v}\right)\right]|w_n|^2+\frac{1}{2}\sin\left(2\omega\frac{l}{v}\right)\sum_{n=0}^{\infty}\sin\left(2\Omega_n\frac{L}{v}\right)$$
$$\times[\mathrm{Im}(w_n w_{n+1}^*)\cos\varphi-\mathrm{Re}(w_n w_{n+1}^*)\sin\varphi] \tag{2}$$

to detect the atom in state $|e\rangle$ after an interaction time t, which is fixed by the velocity v and the effective size L of the cavity mode. Here $\Omega_n=\sqrt{n+1}\Omega$ where Ω is the vacuum Rabi frequency.

The terms of the first sum of Eq. (2) are proportional to the *probabilities* $|w_n|^2$ whereas in the second sum they consist of real and imaginary parts of the product $w_n w_{n+1}^*$ of neighboring *probability amplitudes*. Hence the second sum contains information about the phase between neighboring photon-number probability amplitudes w_n. Note that a straightforward application fails if one amplitude w_n vanishes.

It is the dependence of P_e on the atomic phase φ that allows us to reconstruct the field state. When we assume that the initial field state is a finite superposition,

$$|\psi\rangle=\sum_{n=0}^{n_{\max}} w_n|n\rangle, \tag{3}$$

of number states, we can determine the coefficients w_n as shown in Ref. [1] by measuring the probability $P_e(t,\varphi)$ for at least two phases φ_μ, where $\mu=1,2$ and at least $n_{\max}$ discrete interaction times t_ν, where $\nu=1,\ldots,n_{\max}$: Two phases are necessary to retrieve information about real *and* imaginary parts of the terms $w_n w_{n+1}^*$. Moreover since there is an arbitrary overall phase factor and the normalization condition, we need at least $2n_{\max}$ independent equations to calculate the $n_{\max}+1$ complex coefficients w_n. The probabilities $P_e(t_\nu,\varphi_\mu)$ for different interaction times t_ν and different phases φ_μ provide via Eq. (2) the necessary equations.

While the different phases are provided by settings of the dephaser D, a wide distribution of interaction times follows from the thermal distribution of the atomic velocities. In addition to the detection of the internal state of the atom after the interaction with the quantized field, we also record the time of flight of each atom through the whole apparatus. From this we can calculate the velocity v of the atom and thereby, via the size of the cavity L, the effective interaction time $t=L/v$. After we have detected enough atoms, we calculate the coefficients w_n by a least-square fit, that is, we minimize the expression

$$f\equiv\sum_{\nu,\mu}\frac{1}{\sigma^2(t_\nu,\varphi_\mu)}\left(P_e(t_\nu,\varphi_\mu;\{w_n\}_0^{n_{\max}})-\frac{n_e(t_\nu,\varphi_\mu)}{n(t_\nu,\varphi_\mu)}\right)^2. \tag{4}$$

Here $n(t_\nu,\varphi_\mu)$ is the number of atoms recorded for the time t_ν and the phase φ_μ and $n_e(t_\nu,\varphi_\mu)$ is the corresponding number of excited atoms. We denote the statistical uncertainty in the transfer rate by $\sigma(t_\nu,\varphi_\mu)=n^{-1/2}(t_\nu,\varphi_\mu)$. Due to various experimental uncertainties that we include in this paper, this minimization method is more stable than the method of Ref. [1] based on linear equations.

What parameters of quantum-state endoscopy determine the set of states we can reconstruct? How many number states is a state allowed to contain for this method to be still successful? We answer these questions by giving a heuristic argument. We note that endoscopy works when we can resolve two neighboring Rabi frequencies $2\sqrt{n+1}\Omega$ and $2\sqrt{n}\Omega$ in Eq. (2). We therefore have to resolve a frequency difference $\Delta\Omega_n\equiv 2(\sqrt{n+1}-\sqrt{n})\Omega\approx n^{-1/2}\Omega$. When we recall the Fourier theorem $\Delta\Omega_n\Delta T\approx 1$, where $\Delta T=t_N-t_1$ denotes the time window in which we make the measurements, we find the estimate

$$n\approx(\Omega\Delta T)^2 \tag{5}$$

for the maximum number of photon states. Hence, the Rabi frequency and the time window ΔT determine the type of quantum state that endoscopy can reconstruct.

Of particular interest is the measurement of a coherent state $|\alpha e^{i\theta}\rangle$ of amplitude α and phase θ and that of a Schrödinger cat state [3,4]:

$$|\psi\rangle=\mathcal{N}\{|\alpha e^{i\theta}\rangle+|\alpha e^{-i\theta}\rangle\}. \tag{6}$$

Here $\mathcal{N}$ is the normalization constant. In the experiment we prepare the coherent state directly by coupling the classical source S to the cavity [3]. The cat state can be prepared by sending an atom through the resonator containing initially a coherent state prepared by S. This atom, prepared in a coherent superposition of $|e\rangle$ and $|g\rangle$ by F, interacts dispersively with the cavity C. The atom is tuned out of resonance by a static electric field applied across the mirrors of C. Both states $|e\rangle$ and $|g\rangle$ correspond to different indices of refraction, and dephase the field in C by different amounts. The initial coherent state is therefore split into two coherent components with different phases. In comparison to the setup shown in Fig. 1 we have to add a second classical field after the cavity, which mixes again states $|e\rangle$ and $|g\rangle$, so that the measurement of the atomic state gives no information about the state in the cavity. The final field state, after atomic detection, is then [3] a quantum superposition of the two coherent states Eq. (6).

Our numerical simulation processes in two steps. First, we simulate the outcome of an actual experiment by making random choices according to the appropriate probabilities P_e. Then, simulating data interpretation, we use these random outcomes in the minimization process to reconstruct the field in C. We use the atomic phases $\varphi_\mu=0,\pi/2,\pi,3\pi/2$, and $N=70$ equally spaced interaction times $t_\nu=(10+30\ \nu/N)\mu$s with $\nu=1,\ldots,N$. We take the value of the Rabi frequency $\Omega=10^5$ rad/s from [2].

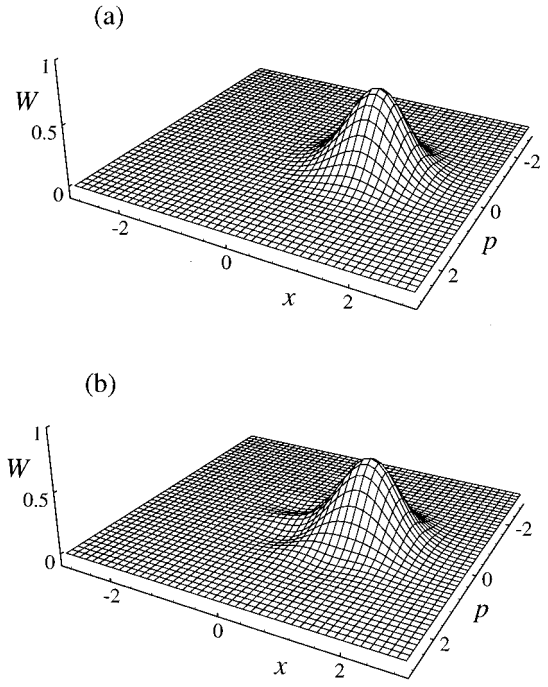

FIG. 2. Reconstruction of a coherent state. Comparison between the Wigner functions of a coherent state with $\alpha=1$ (a) and the reconstructed state (b). The oscillations of the Wigner function of the reconstructed state result from the cutoff $n_{\max}=12$ in the expansion (3) in number states. For the simulation we have used $N_{\mathrm{tot}}=10^5$ atoms. For the remaining parameters, in particular the errors included, see the text.

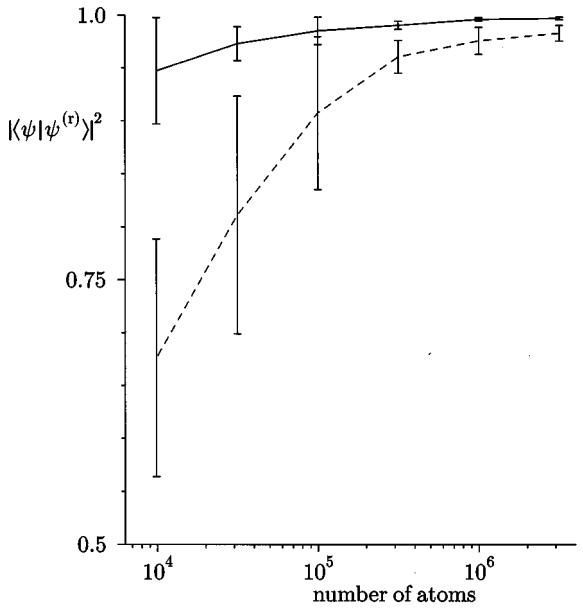

FIG. 3. Quality of the reconstruction of the coherent states $\alpha=1$ and $\alpha=2$ in its dependence on the number of atoms.

In the first stage, the values of the total number of atoms $n(t_\nu,\varphi_\mu)$ in each class is selected, according to the velocity distribution in the beam, and $n_e(t_\nu,\varphi_\mu)$ is obtained by making, for each atom, a random choice between $|e\rangle$ and $|g\rangle$ according to the "true" probability distribution $P_e(t_\nu,\varphi_\mu)$ calculated with the exact cavity field $|\psi\rangle$. At this stage, we also take into account uncertainties in the interaction times t_ν. The atomic velocity is inferred from the time of flight (around 600 μs) through the apparatus. Since the "origin" of time is known within a finite accuracy (a 10 μs laser pulse prepares the Rydberg atoms), the value of the interaction time t_ν deduced from this measurement may differ slightly from the "true" interaction time $t_\nu^{(\mathrm{true})}$, which determines the exact probability distribution P_e. To simulate this effect, we randomly choose for each atom a true time $t_\nu^{(\mathrm{true})}$ uniformly distributed over the interval $[t_\nu-\Delta t/2,t_\nu+\Delta t/2]$ with a width $\Delta t=0.33$ μs. Analogously, we include the effect of the uncertainties $\Delta\varphi$ and $\Delta\omega$ in the phases φ_μ and the classical Rabi frequency ω, respectively. The noise in the atomic phase φ is caused by stray fields, which slightly detune the atom during the flight between F and C. The fluctuations in ω are caused by inhomogeneities of the classical field and the finite width of the atomic beam. In our simulation, we use the values $\Delta\varphi=0.03$ rad and $\Delta\omega/\omega=0.03$ compatible with the experiment of Ref. [2]. We also consider the possibility that the measurement of an atom fails completely. This could be caused by a second atom in the cavity or a bad detection, that is, the detector does not give the true state of the atom. Therefore, we assume that 2% of all atoms are detected in a completely random state.

In the second stage we interpret the data. In particular, we use the results of the simulation, that is the total number $n(t_\nu,\varphi_\mu)$ of atoms recorded for the time t_ν and the phase φ_μ and the corresponding number $n_e(t_\nu,\varphi_\mu)$ of atoms detected in the excited state, to minimize the expression f, Eq. (4), as a function of the photon probability amplitudes w_n. Note that we have to solve this minimization problem subjected to the normalization constraint $\Sigma_{n=0}^{n_{\max}}|w_n|^2=1$. The state obtained in this way reproduces the data of the simulation in the best possible way. We use the so-called dual method for the minimization with constraints [7] summarized in the Appendix. In contrast to many other methods such as the Newton algorithm it provides us with the global minimum without any *a priori* knowledge of the field state. As soon as the dual method has brought us close enough to the global minimum we go over to a faster converging Newton algorithm in order to find the coefficients with high accuracy. This minimization procedure works nicely for coherent states up to an average number $\bar{n}\approx 9$ of photons. This number is governed by Eq. (5) which for the Rabi frequency $\Omega=10^5$ rad/s and the time window $\Delta T=t_N-t_1\approx 30$ μs set by the measurement yields $n\approx 9$.

In Fig. 2 we compare the Wigner function [8] of a coherent state $|\alpha\rangle$ of amplitude $\alpha=1$ with the state obtained via our simulation of quantum-state endoscopy. Here, we have used a total number of atoms $N_{\mathrm{tot}}=10^5$ to probe the field state. The agreement is quite good. As a quantitative measure of the quality of the reconstruction, we use the absolute square of the scalar product of the exact state $|\psi\rangle$ and the reconstructed state $|\psi^{(r)}\rangle$. For the example of Fig. 2, we obtain the value $|\langle\psi|\psi^{(r)}\rangle|^2=0.998$. Let us stress that this excellent reconstruction would be obtained in the actual ex-

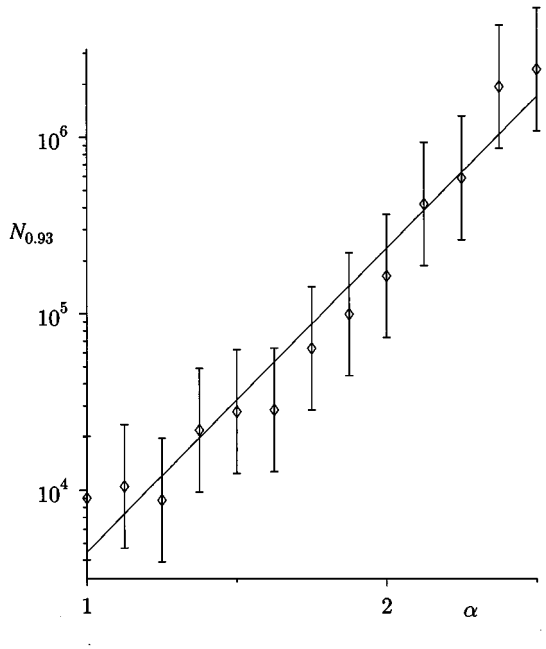

FIG. 4. Dependence of the number of atoms probing the state necessary to achieve a quality 0.93 of the reconstruction on the amplitude of the coherent state $|\alpha\rangle$.

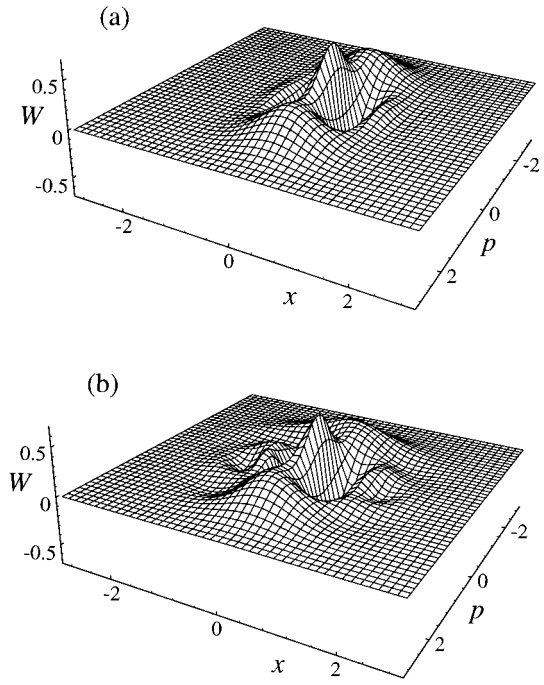

FIG. 5. Reconstruction of a Schrödinger cat via quantum-state endoscopy. Comparison between the Wigner functions of a Schrödinger cat (a) and the reconstructed state (b). Again the oscillations are due to the finite sum of number states with $n_{\max}=14$. Here $\alpha=1.5$ and $\theta=1.47$. The quality of reconstruction is $|\langle\psi|\psi^{(r)}\rangle|^2=0.95$. For the simulation we have used $N_{\text{tot}}=3\times10^5$ atoms.

periment in a time of the order of 1000 s. We can send up to 10^2 atoms/s through the cavity.

In Fig. 3 we show the dependence of $|\langle\psi|\psi^{(r)}\rangle|^2$ and its approach towards unity versus the number of atoms N_{tot}. Moreover, we find an approximately logarithmic dependence of the total number of atoms N_{tot} on the amplitude α to achieve a fixed quality as shown in Fig. 4.

We also reconstruct a Schrödinger cat state, Eq. (6), with the amplitude $\alpha=1.5$ and the phase $\theta=1.47$ rad. In Fig. 5 we show the reconstruction of the Wigner function. Here we obtain the quality $|\langle\psi|\psi^{(r)}\rangle|^2=0.95$.

A problem of our method is to measure states that have vanishing coefficients w_n, like an even Schrödinger cat,

$$|\psi\rangle=\mathcal{N}\{|\alpha\rangle+|-\alpha\rangle\}.$$

Due to the symmetry of this state all even coefficients are zero and consequently it is impossible to recover the phases between neighboring coefficients. To avoid this we add a coherent state $|\alpha_0\rangle$ with the source S and obtain the state

$$|\tilde{\psi}\rangle=\tilde{\mathcal{N}}\{|\alpha_0+\alpha\rangle+|\alpha_0-\alpha\rangle\},$$

which we can measure since all probability amplitudes are then nonzero. The state $|\alpha_0\rangle$, which we add, can first be measured using the same method. Finally, we are able to calculate the state $|\psi\rangle$ from $|\tilde{\psi}\rangle$.

In the same way we can treat any quantum state in which at least one of the probability amplitudes w_{n_0} vanishes. Since the probabilities $|w_n|^2$ are independent of all relative phases our algorithm still provides the correct number statistics. In particular it immediately shows that one number state has vanishing or rather small probability. In that case we know that the reconstructed phase of w_{n_0} and therefore the relative phase between w_{n_0-1} and w_{n_0+1} have large errors. Then we measure the same state but displaced by a known coherent state $|\alpha_0\rangle$ as mentioned above. Hence endoscopy can identify and deal with such problematic states.

We conclude by summarizing our main results. We have presented numerical simulations of quantum-state endoscopy based on experimentally accessible parameters. These simulations take into account uncertainties in the amplitude of the classical field preparing the atomic superposition, in the time of preparation, in the phase of the resulting atomic dipole and include failure of detection. We have shown that this method is very robust and can reconstruct without *a priori* knowledge a coherent state up to nine photons and a Schrödinger cat with amplitude 1.5. This is made possible by finding the global minimum of the expression, Eq. (4), with the help of the dual method. This minimum corresponds to the quantum state of the cavity field, which reproduces the data in the best possible way. Our results clearly show that the time has come for experimental realization of quantum-state endoscopy on Schrödinger cats.

Two of us (P.J.B. and E.M.) thank the Deutsche Forschungsgemeinschaft for support. One of us (P.D.) was supported by the National Scientific Research Foundation of Hungary under Contract No. 017380. This work was partially supported by the EC in the framework of the network program. The Laboratoire Kastler Brossel is Laboratoire de l'Université Pierre et Marie Curie et de l'ENS associé au CNRS.

APPENDIX: METHOD OF MINIMIZATION

Our problem is to minimize the nonquadratic function f, Eq. (4), of the variables w_n with respect to the nonlinear normalization constraint

$$\sum_{n=0}^{n_{\max}} |w_n|^2 = 1. \tag{A1}$$

Many methods such as the Newton algorithm use local Taylor expansions of the function and constraints and therefore yield local minima only. They do not guarantee that the minima obtained are indeed global ones. These methods generally converge fast but depend critically on an initial guess of the position of the global minimum.

In the present paper we use the so-called dual method [7], which provides us with the global minimum without any *a priori* knowledge of its position. We first briefly describe the principle of this method and then apply it to our problem.

In order to minimize a scalar function $f \equiv f(\boldsymbol{x})$ of a n-dimensional real vector $\boldsymbol{x}$ subjected to the vector constraint $\boldsymbol{g}(\boldsymbol{x}) = \boldsymbol{0}$ we have to find [7] the saddle point $(\boldsymbol{x}_S, \boldsymbol{\lambda}_S)$ of the Lagrange function

$$L(\boldsymbol{x}, \boldsymbol{\lambda}) \equiv f(\boldsymbol{x}) + \boldsymbol{\lambda}^T \boldsymbol{g}(\boldsymbol{x}).$$

Here $\boldsymbol{g}$ and $\boldsymbol{\lambda}$ denote m-dimensional real vectors, with $m \leqslant n$ and $\boldsymbol{\lambda}^T \equiv (\lambda_1, \ldots, \lambda_m)$. Therefore the gradients

$$\nabla_{\boldsymbol{x}} L(\boldsymbol{x}, \boldsymbol{\lambda})|_{\boldsymbol{x}=\boldsymbol{x}_S, \boldsymbol{\lambda}=\boldsymbol{\lambda}_S} = \boldsymbol{0}$$

and

$$\nabla_{\boldsymbol{\lambda}} L(\boldsymbol{x}, \boldsymbol{\lambda})|_{\boldsymbol{x}=\boldsymbol{x}_S, \boldsymbol{\lambda}=\boldsymbol{\lambda}_S} = \boldsymbol{g}(\boldsymbol{x}_S) = \boldsymbol{0}$$

of $L(\boldsymbol{x}, \boldsymbol{\lambda})$ with respect to the vectors $\boldsymbol{x}$ and $\boldsymbol{\lambda}$ have to vanish. We note that the vanishing gradient in $\boldsymbol{\lambda}$ guarantees that the vector $\boldsymbol{x}_S$ satisfies the constraint $\boldsymbol{g}(\boldsymbol{x}_S) = \boldsymbol{0}$. Moreover

$$L(\boldsymbol{x}_S, \boldsymbol{\lambda}_S) = \min_{\boldsymbol{x}} L(\boldsymbol{x}, \boldsymbol{\lambda}_S) \tag{A2}$$

must be satisfied. According to the Kuhn-Tucker condition discussed in Ref. [7] the location of the *global* minimum is then $\boldsymbol{x}_S$.

Therefore we now have to find the saddle point $(\boldsymbol{x}_S, \boldsymbol{\lambda}_S)$. For this purpose we employ the dual method. We use two unconstrained optimizations: First we search for the minimum

$$w(\boldsymbol{\lambda}) \equiv \min_{\boldsymbol{x}} L(\boldsymbol{x}, \boldsymbol{\lambda})$$

of the Lagrange function L with respect to $\boldsymbol{x}$ but for fixed $\boldsymbol{\lambda}$. Second we search for the maximum

$$w(\boldsymbol{\lambda}_S) = \max_{\boldsymbol{\lambda}} w(\boldsymbol{\lambda})$$

of the so-called dual function $w(\boldsymbol{\lambda})$. This search for the minimum in $\boldsymbol{x}$ and the maximum in $\boldsymbol{\lambda}$ is motivated by the condition Eq. (A2) specifying the orientation of the saddle point. The $\boldsymbol{x}$ value corresponding to $\boldsymbol{\lambda}_S$ is the global minimum $\boldsymbol{x}_S$. In Ref. [7] it is shown that the dual function is always concave. Hence the maximum of $w(\boldsymbol{\lambda})$ is unique [9].

We now apply this method to our problem and introduce the $(1 + 3n_{\max})$-dimensional vector

$$\boldsymbol{x} \equiv \begin{pmatrix} |w_0|^2 \\ |w_1|^2 \\ \vdots \\ |w_{n_{\max}}|^2 \\ \mathrm{Re}(w_0 w_1^*) \\ \vdots \\ \mathrm{Re}(w_{n_{\max}-1} w_{n_{\max}}^*) \\ \mathrm{Im}(w_0 w_1^*) \\ \vdots \\ \mathrm{Im}(w_{n_{\max}-1} w_{n_{\max}}^*) \end{pmatrix}. \tag{A3}$$

When we denote the mth component of $\boldsymbol{x}$ by x_m the normalization condition, Eq. (A1), reads

$$g_0(\boldsymbol{x}) \equiv \sum_{m=1}^{n_{\max}+1} x_m - 1. \tag{A4}$$

In addition these components have to satisfy the constraints

$$|w_n|^2 |w_{n+1}|^2 = [\mathrm{Re}(w_n w_{n+1}^*)]^2 + [\mathrm{Im}(w_n w_{n+1}^*)]^2,$$

which read in the new variables

$$g_n(\boldsymbol{x}) = x_n x_{n+1} - x_{1+n_{\max}+n}^2 - x_{1+2n_{\max}+n}^2, \tag{A5}$$

where $n = 1, \ldots, n_{\max}$. Note that due to the $1 + n_{\max}$ constraints, Eqs. (A4) and (A5), the number of degrees of freedom remains $2n_{\max}$.

The advantage of this particular choice of $\boldsymbol{x}$, Eq. (A3), is that f is now a quadratic and convex function, because P_e, Eq. (2), is linear in $\boldsymbol{x}$, and $\boldsymbol{g}$ is quadratic in $\boldsymbol{x}$. Consequently the minimum of L with respect to $\boldsymbol{x}$ is unique and easy to find.

[1] P. J. Bardroff, E. Mayr, and W. P. Schleich, Phys. Rev. A **51**, 4963 (1995)

[2] M. Brune, P. Nussenzveig, F. Schmidt-Kaler, F. Bernardot, A. Maali, J. M. Raimond, and S. Haroche, Phys. Rev. Lett. **72**, 3339 (1994); M. Brune, S. Haroche, V. Lefevre, J. M. Raimond, and N. Zagury, *ibid.* **65**, 976 (1990).

[3] M. Brune, S. Haroche, J. M. Raimond, L. Davidovich, and N. Zagury, Phys. Rev. A **45**, 5193 (1992).

[4] W. Schleich, M. Pernigo, and Fam Le Kien, Phys. Rev. A **44**, 2172 (1991).

[5] R. G. Hulet and D. Kleppner, Phys. Rev. Lett. **51**, 1430 (1983); A. Nussenzveig, J. Hare, A. M. Steinberg, L. Moi, M. Gross,

and S. Haroche, Europhys. Lett. **14**, 755 (1991); P. Nussenzveig, F. Bernardot, M. Brune, J. Hare, J. M. Raimond, S. Haroche, and W. Gawlik, Phys. Lett. **48A**, 3991 (1993); R. J. Brecha, G. Raithel, C. Wagner, and H. Walther, Opt. Commun. **102**, 257 (1993).

[6] For the measurement of the density matrix using k-photon transitions see W. Vogel, D.-G. Welsch, and L. Leine, J. Opt. Soc. Am. B **4**, 1633 (1987).

[7] See, e.g., M. Minoux, *Mathematical Programming* (Wiley, Chichester, 1986).

[8] M. Hillery, R. F. O'Connell, M. O. Scully, and E. P. Wigner, Phys. Rep. **106**, 121 (1984).

[9] If the minimum of L with respect to $\boldsymbol{x}$ is unique for $\boldsymbol{\lambda}=\boldsymbol{\lambda}_S$, then according to Ref. [7] the dual function is differentiable at $\boldsymbol{\lambda}=\boldsymbol{\lambda}_S$. This property leads to a great simplification of the minimization procedure.